

Analysis of the changes in the distinguishing features in electroencephalogram signal processing for heroin addicts

Atefeh Tobieha^{1,2} , Neda Behzadfar^{1,2} , Mohammad Reza Yousefi^{1,2,*} ,
Homayoun Mahdavi-Nasab^{1,2} , Ghazanfar Shahgholian^{1,2} 

¹Department of Electrical Engineering, Najafabad Branch, Islamic Azad University, Najafabad, Iran.

²Smart Microgrid Research Center, Najafabad Branch, Islamic Azad University, Najafabad, Iran.

*Corresponding author: mr-yousefi@iaun.ac.ir

Original Research

Received:
19 November 2024
Revised:
18 January 2025
Accepted:
1 February 2025
Published online:
1 March 2025

© 2025 The Author(s). Published by the OICC Press under the terms of the [Creative Commons Attribution License](https://creativecommons.org/licenses/by/4.0/), which permits use, distribution and reproduction in any medium, provided the original work is properly cited.

Abstract:

Heroin is a highly addictive drug with devastating effects on various parts of the body, including the digestive system, nervous system, and mental health, and it can lead to premature death. One of the most destructive impacts of heroin use is on the brain. Electroencephalograms (EEG) indicate the brain's activity in the physiological and psychological states of heroin addicts. Identifying distinguishing features is crucial for processing these signals and determining the differences between the EEGs of healthy individuals and addicts. The frequency and time domain features extracted from different channels of EEG vary, but identifying distinguishing features can aid in better analysis of these signals. This article uses the Davies-Bouldin criterion to determine distinguishing frequency and time domain features. EEGs of heroin addicts (15 individuals) and healthy individuals (15 individuals) were extracted from 16 different channels. The distinguishing feature with the lowest Davies-Bouldin index value was selected. The results of this study show that in people addicted to heroin, the frequency power spectrum in the upper alpha subband of the O1 channel has decreased. Additionally, approximate entropy is increased in the Cz channel of heroin addicts. To evaluate the distinguishing features, support vector machine classification has been used to distinguish addicts from healthy individuals. The sensitivity and accuracy of distinguishing an addicted person from a healthy person in the approximate entropy feature are 91.50% and 91.81%, respectively, and in the power spectrum feature in the upper alpha subband of the O1 channel, they are 95.92% and 92.40%, respectively. Compared to other studies, the obtained results confirm the distinction and superiority of these features in terms of precision and accuracy. According to the results, the analysis of frequency and time domain features of brain signals can help to better understand the effects of heroin consumption on brain activity. This study may help provide solutions to improve the treatment and prevention of heroin addiction.

Keywords: Power spectrum; Distinctive features; Electroencephalogram signal; Heroin; Brain signal processing

1. Introduction

The consumption of narcotics, by affecting neurotransmitters in various brain regions, particularly the reward area, leads to feelings of pleasure, which subsequently induces changes in other areas and functions of the brain. Diamorphine, or heroin, is a highly addictive narcotic derived from morphine, typically seen as a white or brown powder. Long-term heroin addiction extensively impacts an individual's body and life, causing sexual and psychological disorders, gastrointestinal issues, liver and kidney problems, and damage to heart, vascular, and brain health. In 2019 alone, heroin and other potent narcotics led to the deaths of over 130,000 people worldwide. Heroin use significantly impacts

an addict's brain, impairing their ability to properly interact with their surroundings [1].

EEG processing for addiction treatment is one of the effective ways to respond to this complex challenge [2, 3]. Numerous studies have been conducted to identify distinguishing features or affected areas resulting from heroin use. The first step in EEG processing involves recording the signals. After recording and storage, pre-processing is a critical phase, as the signals are undoubtedly influenced by noise and external interferences [4]. Once the EEG is cleared of artifacts and interferences, feature extraction is performed due to the vast amount of electroencephalogram (EEG) signal data collected [5, 6]. The aim of feature extraction is to

reduce the amount of data by creating new features from the initially measured dataset. The extracted features contain pertinent information for diagnosis or treatment [7, 8]. Feature extraction occurs in the time domain, frequency domain, or time-frequency and nonlinear domains [9]. Some studies have assessed the differences in the power spectrum frequency between healthy individuals and heroin addicts using various statistical methods [10, 11]. Frequency analysis is among the efficient methods in this field [12, 13].

In [14], the P300 component was examined in heroin addicts, individuals who had quit heroin, and healthy individuals during a short-term memory test. The addicted individuals exhibited higher impulsivity, which manifested as abnormalities in the P300 component response time. In [15], the P300 component of EEG signals from individuals attempting to quit heroin was analyzed to identify and classify heroin addicts, utilizing these results in deep learning-based classifiers. In [16], the P300 component of event-related potentials (ERP) in healthy individuals and heroin addicts was studied, using a genetic algorithm for feature selection. In [17], the P300 component in EEG signals was examined in ten Heroin addict and ten healthy individuals. In [18], the EEG signals of heroin addicts showed a decreased alpha-to-theta power ratio in the T6 region. In [19], the differences in the beta subband (12 – 22 Hz) and the physiological or operational relationships between different EEG bands in heroin addicts were explored. In [20], a direct correlation between the lower alpha subband in the central brain region (C3, C4, and Cz channels) and the duration of heroin abuse was observed, particularly in the right hemisphere (C4 channel). In [21], the relative power and central frequency of EEG subbands in heroin addicts were compared to those of healthy individuals, specifically in the alpha and beta subbands. In [22], transcranial magnetic stimulation and electroencephalography (TMS-EEG) were used to examine cortical plasticity characteristics in individuals with heroin use disorder compared to healthy individuals.

EEG studies have shown that heroin addicts exhibit low-voltage background activity with reduced alpha rhythm, increased beta activity, and heightened low-amplitude theta and delta waves in central regions. In [23], after extracting the P300 component, a multi-resolution wavelet transform was applied. The results indicated that the P3 channel more significant changes in the wavelet transform for Heroin addict. In [24], the power spectrum of the P300 and P600 components was analyzed. The results indicate that the power spectrum in the alpha 2 subband in the frontal and central regions is greater than in other areas, showing a significant difference between healthy individuals and addicts in these regions. In [25], the changes in the P300 component of EEG signals recorded from addicts and healthy individuals who have used methadone were investigated. This study employed wavelet transform to examine the P300 component, revealing that the P300 component of methadone users significantly differs from that of healthy individuals. In [26], nonlinear features in the alpha subband at rest were examined in individuals who had quit heroin compared to a healthy group. It was found that irregular neuron oscillations in individuals who had quit heroin result in

higher nonlinear dynamics. In the study conducted in [27], the Montreal Cognitive Assessment and statistical analysis with a significance level of 0.05 were used. The results showed a significant difference in EEG between Heroin addict and healthy individuals. In [28], disruptions in the anterior cerebellum and prefrontal circuits were observed in heroin-dependent individuals, indicating an imbalance between local neural activity and neural network connectivity. Table 1 compares studies conducted in the field of frequency domain feature analysis. These studies have examined frequency domain features, such as the power spectrum or the P300 component alone, which may have overlooked some important information necessary for distinguishing between healthy individuals and addicts. Given the dynamic nature of EEG, it is essential to consider time domain features as well. Research shows that the P300 component differs among heroin addicts, individuals who have quit heroin, and healthy individuals during short-term memory tests.

The study in [29] examined the coherence of EEG power in 18 heroin-dependent individuals and 12 healthy controls. The results indicate that heroin-dependent individuals have higher relative beta 2 power and gamma coherence in the left hemisphere compared to the control group. In [30], focusing on the temporal dynamics and frequency characteristics of EEG signals, the amplitude of low-frequency fluctuations (ALFF) was compared between addicts and healthy individuals.

The results show a significant positive correlation between increased ALFF and the dose of methadone used, suggesting that reduced ALFF is associated with heroin use.

A study [31] investigated the relative power and central frequency of the alpha (α) and beta (β) subbands in both addicts and healthy individuals. Significant differences were observed in these features. The analysis of EEG signals revealed that over 70% of cases showed relatively low alpha subband activity, increased beta activity, and a notable amount of low-amplitude waves in the central brain regions. In [32], the effects of heroin on the brain were evaluated by studying the relationships between the power spectrum, average EEG frequency, and the duration of heroin use. The findings indicate that changes in alpha 2 subband frequency are more pronounced in the frontal and central areas and are associated with the duration of heroin use. A decrease in the average frequency of the alpha 1 subband was more prominent in the central, temporal, and axial regions, mainly observed in heroin addicts using high doses of the drug. The power spectrum of brain electrical activity in patients corresponds with the duration of addiction recovery. The results suggest that heavy heroin use causes changes in neural oscillation frequency.

Table 2 summarizes the comparison of studies on the effects of EEG signal changes. Although various features for linear and nonlinear frequency characteristics have been considered. The main challenge remains the inefficiency of the Fourier transform for analyzing dynamic signals. To address this, several studies have divided EEG signals into short, overlapping time intervals. However, it seems that time-domain features may offer a more effective approach for analyzing these signals.

Table 1. Comparison of research background in frequency domain characteristics.

Subject	Ref.	Method	Results	Method Drawback
P300 Component Analysis	[14]	Analysis of addicts during and after treatment, examining various disorders.	Only examined P300 amplitude data	Limited to the P300 amplitude data
	[15]	Use of P300 component for classification through deep learning	Only examined P300 amplitude data	Limited to the P300 amplitude data
	[16]	A comprehensive study of individuals on the P300 ERP component, feature selection	Small sample size and limited generalizability	Small sample size and limited generalizability
	[17]	A comprehensive study of Heroin addict	Only examined P300 amplitude data	Limited to the P300 amplitude data
	[23]	A comprehensive study of Heroin addict	Only applied wavelet transform to the P300 component	Limited to wavelet transform application on P300
	[25]	Study of Heroin addict undergoing methadone treatment.	Only examined the P300 component; statistical tests were incomplete.	Incomplete statistical tests on the P300 component
Relative Power Analysis	[18]	Analysis of all subbands to determine differences between healthy individuals and addicts	Considered only one power spectrum feature	Limited to one power spectrum feature
	[19]	Analysis of all subbands to determine correlations	Only examined central frequency feature	Limited to central frequency feature
	[24]	Analysis of all head regions across all subbands	Limited to one feature examination	Limited to one feature examination
Subband and Channel Comparison	[20]	Analysis of physiological and operational relationships between bands.	Only examined differences in the beta subband.	Limited to beta subband analysis.
	[21]	Analysis of the relationship between the Wechsler Adult Intelligence Scale and EEG signal power changes	Only displayed disruptions in the right hemisphere, not the left	Did not consider left hemisphere disruptions
	[22]	Analysis of drug effects on EEG channels in the cortex, examining all head regions across all subbands	Compared to differences with evoked potentials, the low-voltage background feature was ineffective.	Ineffective low-voltage background feature
	[26]	Comprehensive identification of affected areas in this study	Examined connectivity in all brain regions, limited to the alpha subband	Limited to alpha subband analysis
	[28]	Utilized a genetic algorithm for feature selection and classification of healthy individuals versus addicts	Detected an imbalance between local neural activity and neural network connectivity	Only one type of feature was extracted, and the feature selection focused primarily on dimensionality reduction.
Statistical Comparison	[27]	Demonstrated the correlation between local neural activity and neural network connectivity	Did not consider the functional correlation of brain regions with each other	Did not consider inter-regional brain function correlation

This paper aims to identify appropriate and distinctive features that differentiate addicts from healthy individuals, using a feature selection method. The innovations of this study include:

- Identifying distinguishing features for detecting addiction in EEG

- Exploring both time-domain and frequency-domain features to highlight distinguishing characteristics

Based on the research conducted and the results obtained, there is still no consensus on the type of distinguishing feature. Therefore, the goal of this paper is to select appropriate and distinguishing features among addicts and healthy individuals. The structure of the paper is as follows: In section 2, the research database will be reviewed. In section 3, the proposed method for selecting distinguishing features in healthy and addicted individuals will be presented. Section 5 will cover the evaluation and analysis of the results. Finally, section 6 will provide the conclusions and recommendations.

2. Database

This study utilized a database of EEG signals from both addicts and healthy individuals [33]. The database includes

EEG signals recorded from 16 channels based on the international 10 – 20 system. Electrode placement (as shown in Fig. 1) involved referencing the right ear and grounding to the frontal channel (Fpz), with a sampling frequency set at 256 Hz. It is worth noting that the EEG signals were recorded using the gUSBamp device, manufactured by g.tec Medical Engineering GmbH.

In this investigation, 15 addicts who were in the process of quitting heroin and 15 healthy individuals with no history of drug, alcohol use, or smoking participated voluntarily and consciously. All participants were male and right-handed, and each provided informed consent before participating in the study. Following this, both groups completed the 28-item General Health Questionnaire (GHQ-28). Additionally, the addicts were asked to complete the 45-item Heroin Craving Questionnaire (HCQ-45), designed to assess their craving and desire related to heroin addiction. This questionnaire evaluates the extent of drug dependency and confirms addiction status. It includes questions addressing physical symptoms, anxiety/insomnia, social functioning impairment, severe depression, mood disorders, anxiety disorders, childhood disorders, and other related issues. Participants with psychiatric disorders or a genetic/family

Table 2. Differences in EEG signals between healthy individuals and addicts.

Ref.	Method	Results	Method Limitation
[29]	Examination of the coherence of the power spectral density of EEG to determine differences between hemispheres	Examined all subbands to determine differences between healthy and addicted individuals in the hemispheres	Only the coherence of the power signal was examined (one feature is not sufficient)
[30]	Dynamics and frequency characteristics of EEG signals	Examined differences in time and frequency domain characteristics across all head points and brain areas Examined the impact of drug use on addicts and healthy individuals	Did not determine the amount of methadone used for treatment
[31]	Examination of relative power and central frequency of alpha and beta subbands	Examined two features simultaneously in the frequency domain	Differences were examined in only two subbands between healthy and addicted individuals
[32]	Examination of the relationship between power spectrum and mean frequency of EEG and duration of heroin use	- Examined drug-related disorders in the treatment process- Examined all subbands to determine the relationship	Only one feature was considered for the relationship analysis
This study	Determination of distinguishing features in the time and frequency domain	Investigating all subbands and channels in both frequency and time domain features- Determined the heroin in the brain affected - Applied an appropriate method for determining distinguishing features	Did not determine the relationship between brain regions in the examined frequency and time domain features

history of neurological conditions were excluded from the study. Table 3 provides further details about the participants.

It is important to note that EEG recordings were made in a low-light room with minimal head movement. For the addicted participants, the last consumption of heroin occurred at least three days before the EEG recording. Additionally, records of epilepsy and the use of psychotropic drugs were taken into account.

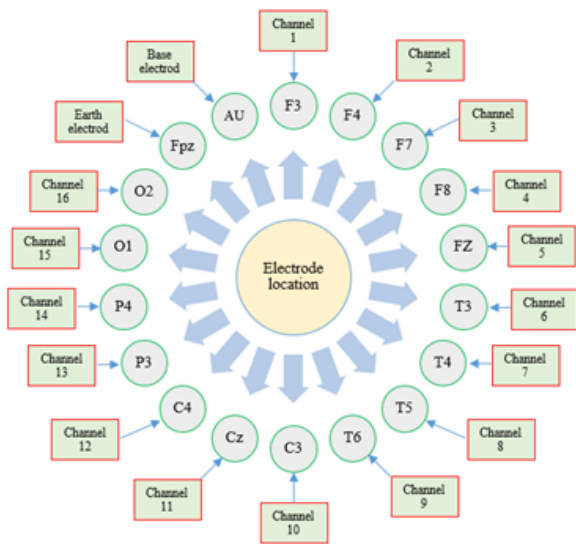


Figure 1. Electrode Placement.

3. Proposed method

The block diagram of the proposed method is shown in Fig. 2. As illustrated, the proposed method includes pre-processing, feature extraction, and feature evaluation. Each section is briefly explained as follows.

3.1 Preprocessing

MATLAB software was used to process and analyze the recorded data. Initially, a 50 Hz notch filter was applied to remove power line noise. Subsequently, a Butterworth band-pass filter with a range of 0.4 to 45 Hz and a 6th-order filter were used to eliminate additional noise.

3.2 Extracted features

In this study, both frequency and time domain features were extracted to identify distinguishing characteristics. Time domain features include permutation entropy (*PE*), approximate entropy (*ApEn*), wavelet entropy, Petrosion fractal dimension, Katz fractal dimension, box-counting fractal dimension, and frequency domain features such as power spectrum in various sub-bands. Approximate entropy measures the regularity and variability in time series data by comparing similar patterns within the data vector. A sample vector of dimension *mmm* is defined as a sliding window of the signal, as follows:

$$u[i] = [x[i]x[i + 1] \dots x[i + m - 1]]^T \tag{1}$$

where $u[i]$ is the output after windowing, $x[i]$ is the input signal, *mmm* is the window length, and *iii* is the sample index within the defined window. The self-similarity of the vector generated from the signal is defined by $C_{i,m}$ self-similarity based on the window applied to the signal is given by:

$$C_{i,m} = \frac{1}{N - m + 1} \sum_{j=1}^{N-1} \theta(r - \|u(i) - u(j)\|_{\infty}) \tag{2}$$

where $\theta(x)$ is the step function, which is defined by (3).

$$\theta(x) = \begin{cases} 1 & x \geq 0 \\ 0 & x < 0 \end{cases} \tag{3}$$

when *X* has the highest self-similarity, $u(j)$ and $u(i)$ are very close to each other, and the value of will be maximized.

Table 3. Characteristics of participants in the study.

Healthy Controls	Addicts	Attribute
15 Men	15 Men	Number of Participants
38.34 years	32.27 years	Age (Mean)
15 years	8.67 years	Education (Years-Mean)
4 Married, 11 Single	8 Married, 7 Single	Marital Status
-	11.2 years	Duration of Heroin Use (Years-Mean)
-	1.2 grams	Daily Dose of Heroin (Grams-Mean)
-	10.07 days	Duration of Abstinence (Days - Mean)

Based on the calculated parameters, *ApEn* computes the internal similarity index across all possible transitions in the sample vectors, indicating the length and resistance to changes. The approximate entropy *ApEn* is computed using the relation (4) [34]:

$$ApEn(X, m, r) = \frac{1}{N - m + 1} \sum_{i=0}^{N-m} \log C_{i,m}(r) - \frac{1}{N - m} \sum_{i=0}^{N-m-1} \log C_{i,m-1}(r) \quad (4)$$

where $C_{i,m}$ represents the self-similarity, m is the window length, N is the total number of signal samples, and r is the overlap value in the window. Permutation entropy (*PE*) is a measure of the complexity of a signal. For a sample vector $u[i]$ after windowing and a permutation π_k with order m , which includes $m!$ patterns, the probability of a permutation pattern for all $k = 1, 2, \dots, m!$ is defined as the probability of occurrence of a sample vector with similar patterns. Permutation entropy calculates the likelihood that the sample vector has a pattern similar to the permutation pattern. Permutation entropy is defined as follows [35].

$$P(\pi_k) = \frac{1}{N - m + 1} \sum_{i=0}^{N-m} f(u[i]\pi_k) \quad (5)$$

where N is the total number of samples. The following relation applies when $u[i]$ and have similar patterns; otherwise, the value is zero.

$$f(u[i]\pi_k) = 1 \quad (6)$$

In this case, a pattern with order $u[i]$ is defined according to the elements of the original signal. Therefore, *PE* is defined

by relation (7) [36].

$$PE = - \sum_{k=1}^{m!} p(\pi_k) \log(\pi_k) \quad (7)$$

Wavelet entropy expresses the uncertainty of a process by calculating its wavelet transform [37].

$$WEn(X, m, B) = \frac{1}{\log(B)} \sum_{i=1}^B W(p_i) \log(W(p_i)) \quad (8)$$

where W is the discrete wavelet transform applied to the probability distribution function, X is the signal, m is the wavelet transform level, and B is the wavelet transform components. The Katz fractal dimension is a mathematical index that can measure the complexity of a signal [38]. It is a fast algorithm for calculating fractal dimensions and is used to measure signal complexity [39, 40].

$$Lm(T) = \frac{1}{T} \left[\sum_{i=1}^{N-m} |x[m+iT] - x[(i-1)T]| \right] \frac{N-a}{\left[\frac{N-m}{T} \right] T} \quad (9)$$

where x is the EEG, the partial time series over the time interval T , and the start time m for $m = 0, 1, 2, \dots$ are calculated. N is the total number of samples in a signal. The fractal dimension method, similar to a box-counting method, acts as a perimeter measurement method, where the signal is covered by a grid. The line length, sometimes considered the curve length, is the overall vertical length of the signal used to calculate the fractal dimension of the signal. Fig. 3 shows the type of calculation for this method.

The Petrosian fractal dimension is a fast algorithm for calculating fractal dimension, operating more quickly than the Katz fractal dimension. This fractal dimension is computed from a binary sequence, so the first step is to convert the input signal into a binary sequence, for which various methods exist. To calculate the Petrosian fractal dimension, the difference between consecutive samples is calculated, and based on whether the calculated value is greater or less than the standard deviation of the window, it is assigned a value of one or zero, respectively. Finally, the fractal dimension is calculated from the binary sequence as follows [42, 43]:

$$D = \frac{\log_{10}(n)}{\log_{10}(n) + \log_{10}\left(\frac{n}{n+0.4N_D}\right)} \quad (10)$$

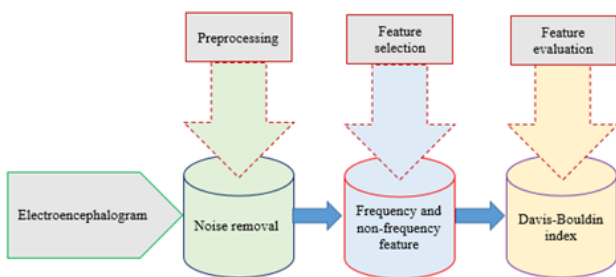


Figure 2. Block diagram of the proposed method.

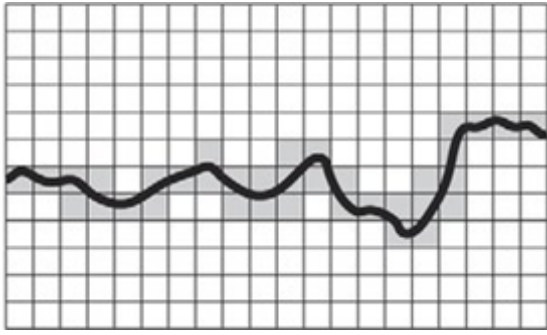


Figure 3. Illustration of the box-counting method by counting the black rectangles [41].

where n is the length of the signal (number of points) and N_D represents the number of sign changes (number of dissimilar pairs) in the generated binary sequence. In the frequency domain, the power spectrum feature in each sub-band can be used. EEG signals are typically identified and examined in four frequency bands: delta (0 – 4 Hz), theta (4 – 8 Hz), alpha (8 – 13 Hz), and beta (15 – 30 Hz), along with the sensory-motor rhythm (12 – 15 Hz). EEG is unique for each individual. Therefore, calculating the individual alpha frequency (IAF) and transition frequency (TF) can be used for more precise analysis.

In physiological studies, the EEG power spectrum reflects the number of neurons firing simultaneously. The power spectrum of the signal is obtained from the Fourier transform of the EEG. Based on the overlap and Welch's method, the power spectral density is calculated using the following relation [44]:

$$P_{XX}^{(i)}(f) = \frac{1}{LU} \left| \sum_{n=0}^{L-1} W(n)X_i(n)e^{-j2\pi fn} \right|^2 \quad (11)$$

where $W(n)$ is the window, L is the window length, and x is the segment of the signal within the window. U is the window normalization factor and is calculated as follows:

$$U = \frac{1}{L} \sum_{n=0}^{L-1} W^2(n) \quad (12)$$

The signal power using Welch's method is calculated by the following formula:

$$P_{XX}^i(f) = \frac{1}{K} \sum_{i=0}^{K-1} P_{XX}^{(i)}(f) \quad (13)$$

The amplitude of the EEG signal for each person depends on various factors such as the anatomical and physiological characteristics of the brain, surrounding tissues, and electrode impedance. These factors vary for each individual and cause significant variations in the absolute power spectrum of the EEG signal. To compensate for these variations, the relative power spectrum is calculated as follows:

$$P_r(f) = \frac{P_a(f)}{\sum P_a(f_i)} \quad (14)$$

where $P_r(f)$ relative is power spectrum at frequency f , and $P_a(f)$ is the absolute power spectral density at the same

frequency. Research has shown that the frequency sub-band ranges of EEG are unique to each individual and vary from person to person; therefore, the frequency range of each sub-band should be calculated separately for each individual [45]. In most individuals, after closing their eyes and being in a state of alertness, the alpha rhythm becomes dominant. When a person opens their eyes and does not engage in any specific mental activity, the alpha rhythm is blocked, and no dominant spectrum is observed in the EEG. By obtaining the baseline EEG of an individual in both the eyes-closed and eyes-open states, the frequency range where the power spectrum of the eyes-closed state diverges from that of the eyes-open state can be identified. With this identified frequency range, the individual alpha peak (IAP) for each person can be calculated as follows:

$$IAP = \frac{\sum_{f=f_1}^{f=f_2} P_r(f) \times f}{P_r(f)} \quad (15)$$

where $P_r(f)$ represents the power spectrum of the signal, f is the frequency in hertz, and f_1 and f_2 are the lower and upper frequencies of the extracted alpha range for each person. After calculating the IAP and TF for each individual, the range from $TF - 2$ Hz to TF Hz is considered the theta sub-band, TF to $IAP - 2$ Hz as the individual's lower alpha sub-band, $IAP - 2$ to IAP Hz as the second lower alpha sub-band, and IAP to $IAP + 2$ Hz as the upper alpha sub-band.

3.3 Davis-Bouldin index

In this analysis, the Davis-Bouldin index is used to evaluate the extracted features. In this index, the similarity between two features R_{ij} is defined based on the dispersion of features S_i and S_j . The similarity between the two features is defined as follows [46]:

- 1) $R_{ij} \geq 0$
- 2) $R_{ij} = R_{ji}$
- 3) If S_i and S_j are both zero, then R_{ij} is also zero.
- 4) If $S_j > S_k$ and $d_{ij} = d_{ik}$ then $R_{ij} > R_{ik}$
- 5) If $S_j = S_k$ and $d_{ij} < d_{ik}$ then $R_{ij} > R_{ik}$

Typically, the similarity between two features is defined as follows:

$$R_{ij} = \frac{S_i + S_j}{d_{ij}} \quad (16)$$

where S_i and S_j represent the dispersion matrices of the i -th and j -th features, respectively, which are calculated using the following equations.

$$d_{ij} = d(V_i, V_j) \quad (17)$$

$$S_i = \frac{1}{\|C_i\|} \sum_{x \in C_i} d(X, V_i) \quad (18)$$

Based on the aforementioned information and the definition of similarity between two features, the Davis-Bouldin index is defined as follows:

$$DB = \frac{1}{n_c} \sum_{i=1}^{n_c} R_i \quad (19)$$

where R_i is calculated as follows:

$$R_i = \max(R_{ij}), i = 1, \dots, n_c, j = 1, \dots, n_c \quad (20)$$

This index essentially calculates the average similarity between each feature and the most similar feature to it. In fact, the higher the value of this index, the better the feature produced.

In this paper, the Davies-Bouldin criterion is used to evaluate the extracted features. In this index, the similarity between two features is defined based on the dispersion of the features. The index calculates the average similarity between each feature and its most similar counterpart. Essentially, the lower the value of this index, the better the feature separation. This feature selection method ensures that the defined selection index condition is symmetric and non-negative. The index calculates the similarity between each cluster and its most similar cluster, averaging the result across all clusters. As a result, it helps to select the most distinctive features.

4. Results

In order to analyze EEG signals, time domain characteristics such as approximate entropy (app_entro), wavelet entropy (wave_entro), permutation entropy (permant_entro), Katz's fractal dimension (Katz), Petrosian's fractal dimension (Petrosion), and box count (box count) in different channels, as well as the frequency characteristics of the relative power spectrum in various subbands, have been extracted from all channels. These features are then used to differentiate between groups. For evaluation, these characteristics were calculated for all participants and compared using a box diagram. The box plots illustrate the differences in the extracted frequency characteristics across different subbands. Fig. 4 shows the differences between time domain features in all channels, with the comparison based on the Davies-Bouldin criterion. The significance threshold is set at 0.005. There is no significant difference in channels 10, 14, 15, and 9, while an increase in the value of the Davies-Bouldin index is evident in addicted individuals. The time domain feature distinguished from other features based on

the Davies-Bouldin value is the approximate entropy in the Cz channel (channel number 11), with a numerical value of 5.22. Fig. 5 presents a similar evaluation for frequency features, which have shown a decrease in heroin addicts. A significant difference has been observed in the upper alpha subband in channel O1 (channel number 15). Table 4 provides labels for Fig. 5. In Table 4, lower2_healthy indicates the second lower alpha subband of healthy individuals, lower2_heroin addict indicates the second lower alpha subband of heroin-addicted subjects, lower1_healthy indicates the first lower alpha subband of healthy individuals, lower1_heroin addict indicates the first lower alpha subband of heroin-addicted subjects, upper_healthy indicates the upper alpha subband of healthy subjects, upper_heroin addicted indicates the upper alpha subband of heroin-addicted subjects, smr_healthy indicates the sensory motor rhythm of healthy subjects, smr_heroin addicted indicates the delta subband of healthy subjects, delta_heroin addicted indicates the delta subband of heroin-addicted subjects, theta_healthy indicates the theta subband of healthy subjects, and finally, theta_heroin addicted indicates the theta subband of heroin-addicted subjects.

5. Discussion

The comparison is based on the Davis-Bouldin index, with a significance level of 0.005. No significant differences were observed in channels 10, 14, 15, and 9, though an increase in the Davis-Bouldin index was noticeable among individuals with addiction. The most distinguished time domain feature, according to the Davis-Bouldin index, was Approximate Entropy in channel Cz (number 11) with a value of 5.22. Fig. 5 shows the evaluation of frequency features, indicating a decrease in this feature among addicted individuals. Significant differences were observed in the upper alpha sub-band in channel O1 (number 15). References [29] to [32] confirm the significant impact of heroin use on the brain. Based on this study, the results,

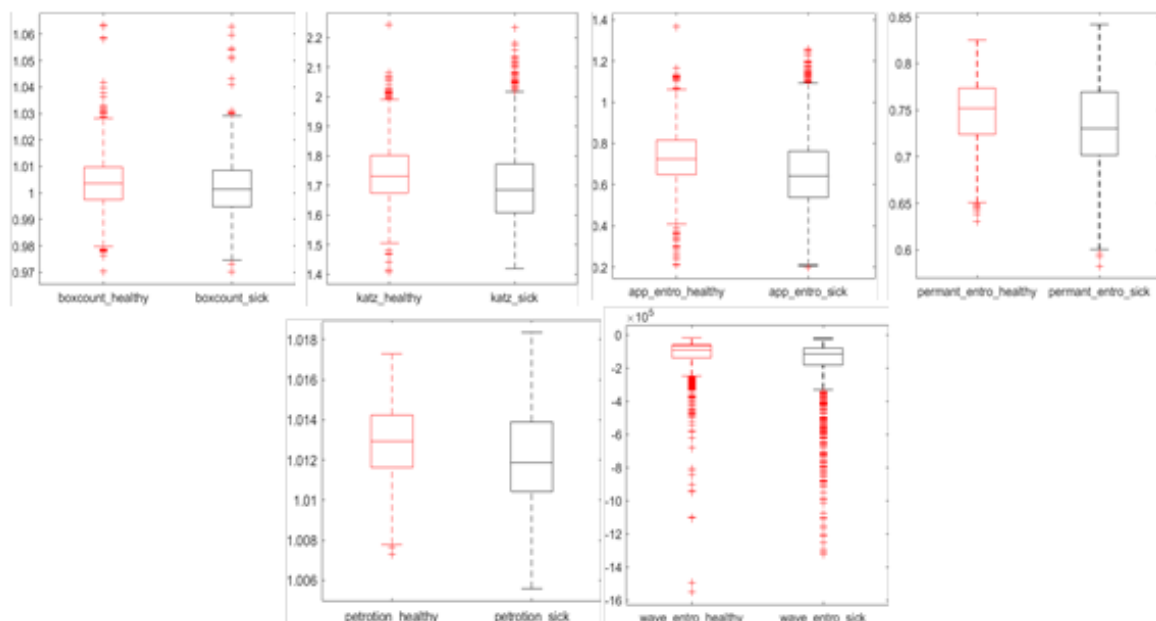


Figure 4. Comparison of time domain features across all channels.

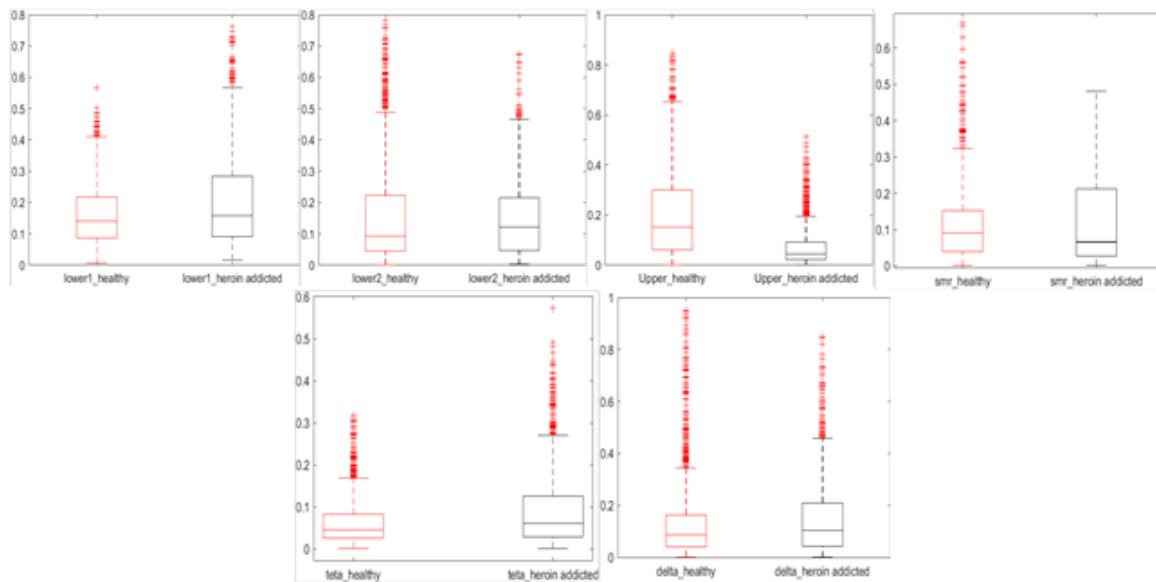


Figure 5. Comparison of power spectrum across different subbands.

and the charts presented in Fig. 4, significant differences in time domain features were observed only in Approximate Entropy. Other time domain features such as Permutation Entropy, Wavelet Entropy, Petrosian Fractal Dimension, Katz Fractal Dimension, and Box Counting Dimension either did not show significant differences or were not notable enough to be used as distinguishing features.

The results for Approximate Entropy align with expectations, as drug use, particularly heroin, increases disorganization in the thoughts of users. Fig. 6 shows the values obtained for Approximate Entropy across all different channels. According to the results presented in this figure, the Davis-Bouldin index shows significant differences in three channels, while the remaining 13 channels exhibit substantial differences, with channel 11 (Cz) showing the greatest significant difference.

Fig. 7 compares various sub-bands, including upper alpha, first lower alpha sub-band, second lower alpha sub-band, sensorimotor rhythm (SMR), theta sub-band, and delta sub-band across 16 channels. The results indicate a significant difference in the upper alpha sub-band, with the most pronounced difference observed in channel 15 (O1). Numerical

comparison results are shown in Fig. 7. In this research, both frequency and time domain features were evaluated using the Davis-Bouldin index. The power spectrum in the upper alpha band at channel O1 (channel 15) had the lowest Davis-Bouldin index value of 1.94. In the research conducted by Saif et al., the evaluation using the Davis-Bouldin index showed an increase in power spectrum across all channels, whereas a decrease in power spectrum was observed in channel Fz. For selecting distinguishing features, the lowest Davis-Bouldin index value is more effective. Therefore, in this study, channel O1 with a Davis-Bouldin value of 1.94 is suggested as the most distinguishing frequency feature. Based on the authors' studies, there has been no comprehensive research on time domain features. This research identifies the most distinguishing feature as the approximate entropy in channel Cz (channel 11) with a Davis-Bouldin value of 5.22.

In order to evaluate the effectiveness of the time domain discriminating features; including approximate entropy, wavelet entropy, per-mutational entropy, Katz fractal dimension, Petrosian fractal dimension, and box-counting fractal dimension; as well as the power spectrum density

Table 4. Description of Fig. 5 labels.

Label	Description
lower2_healthy	Second lower alpha subband of healthy people
lower2_heroin addict	Second lower alpha subband of heroin addicted subject
lower1_healthy	First lower alpha subband of healthy people
lower1_heroin addict	First lower alpha subband of heroin addicted subject
upper_healthy	Upper alpha subband healthy subject
upper_heroin addicted	Upper alpha subband of heroin addicted subject
smr_healthy	Sensory motor rhythm of healthy subject
smr_heroin addicted	Sensory motor rhythm of heroin addicted subject
delta_healthy	Delta subband of healthy subject
delta_heroin addicted	delta subband of heroin addicted subject
Teta healthy	Theta subband of healthy subject
teta_heroin addicted	Theta subband of heroin addicted subject

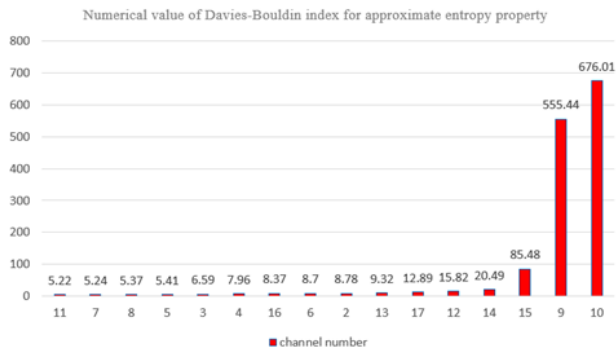


Figure 6. Comparison of Davis-Bouldin index values across all channels for approximate entropy feature.

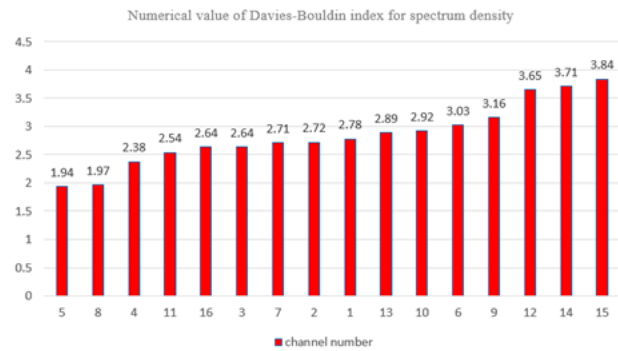


Figure 7. Comparison of Davis-Bouldin index values across all channels for alpha band power spectrum.

feature, another experiment has been designed. In this test, the distinguishing features from the respective channels are classified using a widely used classifier in the field of pattern recognition known as the Support Vector Machine (SVM). The extracted features from different channels are input into the SVM classification model. The classification accuracy is then calculated. Equation (21) computes the accuracy, while equation (22) displays the accuracy value:

$$Precision = \frac{TP}{TP + FP} \times 100 \quad (21)$$

$$Accuracy = \frac{TN + TP}{TN + TP + FN + FP} \times 100 \quad (22)$$

where, *TP* is true positive, *TN* is true negative, *FP* is false positive and *FN* is false negative. Table 5 shows the accuracy and accuracy of classification with support vector machine in different channels and according to different features. 70% of the data in the database is used for training and 30% for testing. Table 5 shows the result of classification in all channels for time domain features. The features extracted in the channels in the database are classified by the support vector machine classifier. As can be seen from the results obtained in Table 5, the support vector machine classifier has the best result in detecting and classifying the addicted person from the healthy person in the approximate entropy feature in channel 11, which is related to the

time domain feature. This feature was determined by Davis Boldin criterion as the best discriminating feature. The classification results have also confirmed this issue. The characteristic of the frequency power spectrum of different subbands in the channels in the database is extracted and categorized by the support vector machine. Table 6 shows the results obtained in this classification. The results of this table show that the upper alpha subband in channel 15 has the highest accuracy and precision in distinguishing addicted maples from healthy ones. By comparing Table 5 and Table 6, it can be concluded that the features of the frequency domain, such as the power spectrum calculated from different subbands, are more effective in distinguishing healthy people from addicts compared to time domain features. Also, the results obtained in Table 6 are consistent with the results obtained in [44] regarding the superiority of the results of classifying and distinguishing addicted people from healthy people in channel 15 or area (O1). In this research, abnormal activities in the occipital, right parietal, temporal, and frontal lobes of drug addicts compared to healthy individuals have been proven. For two differentiating features in time and frequency domains, confusion matrices were reported. Fig. 8 shows the confusion matrix for the approximate entropy feature in channel 11. Fig. 9 shows the confusion matrix for the characteristic of the frequency power spectrum in the upper alpha subband in

Table 5. Classification result in all channels for time domain features.

Channel number	Approximate entropy		Wavelet entropy		Permutation entropy		Katz fractal dimension		Petrosian fractal dimension		Box-counting fractal dimension	
	Precision	Accuracy	Precision	Accuracy	Precision	Accuracy	Precision	Accuracy	Precision	Accuracy	Precision	Accuracy
11	91.55	91.15	87.02	88.28	86.96	87.11	85.25	85.45	80.00	81.12	75.90	75.50
7	89.43	90.52	86.89	88.14	85.88	85.23	83.14	83.02	79.23	80.14	75.02	75.30
8	88.51	90.00	85.19	87.00	85.28	84.85	84.25	84.25	78.25	79.45	74.14	74.79
5	88.32	88.76	84.53	83.89	82.18	83.90	82.72	82.90	78.14	79.02	73.50	73.97
3	87.50	88.37	83.10	83.13	82.89	82.87	80.58	81.56	76.25	78.25	73.14	72.33
4	85.23	88.50	81.33	82.11	82.52	81.90	78.28	79.38	75.78	77.18	72.26	82.89
16	84.42	88.70	80.14	80.19	80.22	80.14	77.79	78.85	74.99	76.10	71.25	72.15
6	84.00	85.10	79.79	80.08	80.00	79.50	76.97	77.08	74.23	75.15	71.01	71.28
2	83.17	85.60	78.88	79.55	78.05	78.45	75.14	75.79	75.26	74.28	70.89	71.02
13	82.99	84.10	77.25	78.15	77.14	78.02	75.50	75.97	75.00	74.18	69.11	71.01
17	82.33	84.15	77.01	77.28	76.20	76.25	73.14	74.33	74.23	74.15	68.01	70.28
12	81.26	83.28	75.89	76.32	75.84	76.18	71.26	72.89	73.26	73.28	67.89	79.32
14	81.00	82.18	74.11	75.01	74.36	74.89	70.19	71.33	73.00	73.18	67.11	69.01
15	80.15	81.17	74.37	74.28	74.80	74.09	70.11	70.18	72.52	73.90	66.26	68.39
9	79.79	81.17	75.02	73.00	73.23	73.36	69.90	70.72	71.22	72.14	65.79	68.75
10	79.74	80.32	71.14	72.05	72.12	73.15	68.88	69.59	70.84	71.50	64.97	66.08

Table 6. Classification result in all channels for frequency spectrum features.

Channel number	Upper alpha band		First lower alpha band		Second lower alpha band		Sensory motor rhythm		Theta subband		Delta subband	
	Precision	Accuracy	Precision	Accuracy	Precision	Accuracy	Precision	Accuracy	Precision	Accuracy	Precision	Accuracy
15	92.95	92.18	91.02	91.77	89.96	89.19	88.25	88.45	89.59	86.12	84.90	85.28
14	92.43	91.58	90.89	90.99	89.88	89.89	88.14	87.55	85.23	86.06	83.02	83.34
12	91.51	91.09	90.19	91.39	88.29	89.85	87.25	87.34	84.25	85.45	82.14	82.79
9	91.32	91.00	89.53	90.89	87.17	88.87	86.72	86.90	83.14	84.02	81.50	81.72
6	90.54	90.37	89.10	89.13	87.01	88.00	85.58	86.56	82.25	82.35	80.14	81.33
10	90.23	90.25	88.33	88.11	86.52	87.90	85.28	85.38	80.54	81.25	79.26	80.26
13	89.42	90.70	88.14	88.00	86.22	87.17	84.79	84.54	79.99	80.01	78.45	79.15
17	88.00	89.10	87.87	87.28	85.84	86.50	83.97	84.08	79.23	79.15	77.78	79.08
2	84.17	86.40	83.88	83.55	85.25	86.45	83.17	83.79	77.26	78.28	77.01	78.23
7	82.99	83.10	82.02	83.15	80.14	84.02	81.50	82.09	76.03	77.89	75.85	76.85
3	81.23	82.15	80.01	81.28	79.25	80.25	80.14	82.33	75.23	76.15	74.51	75.28
16	80.26	81.28	79.89	80.32	78.87	80.18	79.26	81.89	74.26	74.29	73.89	74.32
11	80.08	81.18	78.11	79.01	78.36	79.09	78.19	80.33	72.07	73.18	73.11	73.01
4	79.19	80.17	77.47	78.28	76.80	77.79	77.11	79.18	71.52	71.90	72.28	72.38
8	78.78	79.17	77.05	77.08	76.22	76.36	76.90	78.82	70.22	71.05	70.15	70.99
5	78.74	78.32	76.12	77.00	75.12	75.15	75.87	77.58	69.84	70.11	69.00	70.08

channel 15. For other features, the classification accuracy value is presented in the Tables 5 and 6.

5.1 Comparison with other research

In this section, several studies are reviewed and compared with the findings of this research. The examination of the consistency of electroencephalogram (EEG) signal power in 18 heroin addicts and 12 healthy individuals is presented in [47]. The results indicate that heroin addicts exhibit increased beta 2 relative power and gamma coherence in the left hemisphere compared to the control group.

In [48], the focus is on the time dynamics and frequency characteristics of the EEG signal in individuals with addiction. This study investigates the amplitude of low-frequency fluctuations (ALFF) in addicts compared to healthy individuals. The findings reveal a significant positive correlation between increased ALFF and the dosage of methadone used. Consequently, it can be inferred that a reduction in ALFF is associated with heroin use.

In [49], the relative power and central frequency of the alpha and beta sub-bands have been investigated in addicted people and healthy people. The results of this research show

a significant difference between the desired characteristics. The analysis of the electroencephalogram signal shows that in more than 70% of cases, a relatively low amplitude of alpha subband activity, an increase in beta activity and a significant amount of low-amplitude waves in the central regions of the brain are observed in this feature. to be in [50], the effects of heroin on the brain have been evaluated by studying the relationships between the power spectrum and average frequency of the electroencephalogram and the duration of heroin use.

The research results show that the frequency changes in the alpha 2 subband are more prominent in the frontal and central areas and are related to the duration of heroin consumption. The decrease in the average frequency of the alpha one subband was more prominent in the central, temporal and axial regions, which was mainly observed in heroin addicts who used a high dose of the drug. The power spectrum of brain electrical activity in sick people corresponds to the duration of addiction withdrawal. The results show that high consumption of heroin causes changes in the frequency of neural oscillations. Table 7 summarizes the comparison of the effect of electroencephalogram signal changes in the

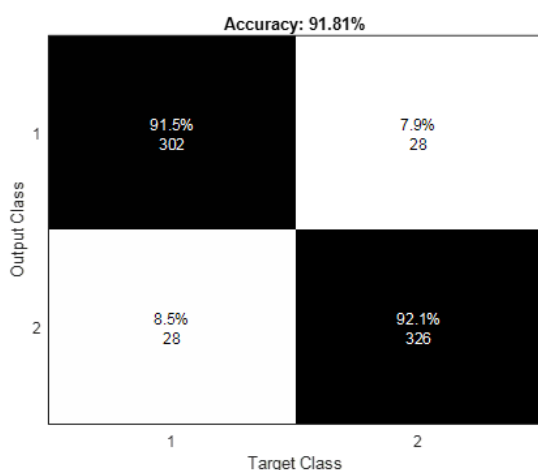


Figure 8. Confusion matrix for the approximate entropy feature in channel 11.

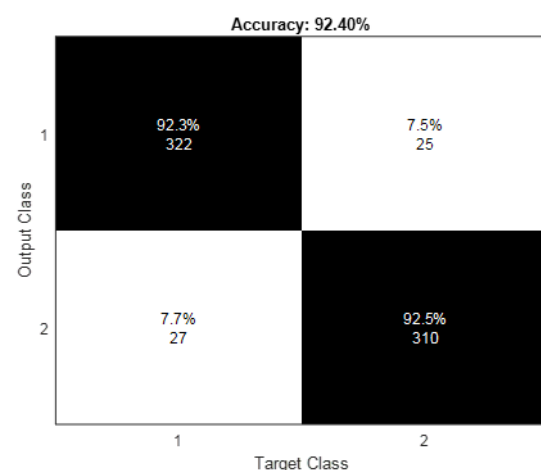


Figure 9. Confusion matrix for the characteristic of the frequency power spectrum in the upper alpha subband in channel 15.

Table 7. Differences between healthy people and addicted people in the electroencephalogram signal.

Ref.	Method	Results	Weak point
[47]	Examining the consistency of brain signal power spectrum density in determining the difference between the two hemispheres	Examining all subbands to determine hemispheric differences between healthy and addicted subjects	Only the signal power uniformity feature is checked (one feature is not enough)
[48]	Dynamics and frequency characteristics of electroencephalogram signal	Investigating the differences in time and frequency domain characteristics in all parts of the head and brain	Failure to determine the amount of methadone used for treatment
[49]	Investigating relative power and center frequency of alpha and beta subband	Investigating the effect of drug use in addicted and healthy people	Examining the differences in healthy and addicted people has been done only in two sub-bands.
[50]	Investigating the relationship between the power spectrum and average frequency of the electroencephalogram and the duration of heroin use	Simultaneous examination of two features in the frequency domain	Only one attribute is considered for correlation analysis.
Proposed method	Determining the distinguishing feature in the time and frequency domain	Examining drug disorders in treatment	Failure to determine the relationship between brain regions in the examined frequency and non-frequency characteristics

conducted studies. Based on the above results, although several features have been considered for linear and non-linear frequency features, however, the main challenge of Fourier transform, i.e. inefficiency for dynamic signals, is raised. To overcome this challenge, in these studies, EEG signals are divided into short and overlapping intervals, but it seems that non-frequency characteristics can be investigated more effectively. The results obtained in this present research are compared with [51] in order to determine the distinguishing feature, in which the support vector machine classification was used to identify the addicted person from the healthy person. The comparison results are shown in Table 8. Based on this table, the superiority of the distinguishing features of this research can be seen compared to the compared method due to confirmation by the Davis-Bouldin test.

This paper tackles challenges related to demonstrating the effectiveness of time-domain features in representing information, as well as addressing the non-stationarity and complexity of brain signals. To achieve this, both time-domain and frequency-domain features were extracted, with the most distinctive features identified using the Davies-Bouldin criterion. Several experiments were designed to validate the resolution of these challenges and gaps. The results indicate that these challenges have indeed been addressed. Additionally, features derived from common domain transforms, such as the wavelet transform, which provides characteristics from both time and frequency domains, have proven beneficial. Employing modeling-based methods could further substantiate the findings presented in this study, potentially reinforcing the conclusions drawn.

6. Conclusion

In this paper, we have meticulously extracted a comprehensive set of both frequency and time domain features from various sub-bands and electrodes to delineate the distinguishing characteristics in the EEG signals of healthy individuals and heroin addicts. Our findings reveal pronounced disparities in several of these features, underscoring the potential of EEG analysis in identifying the neurological impacts of heroin addiction. Notably, in the upper alpha band, there was a marked reduction in the power spectrum observed in channel O1 of the addicts, signifying potential alterations in brain activity associated with addiction. Furthermore, the approximate entropy in channel Cz exhibited a significant increase among the addicts, indicating a higher level of complexity and irregularity in their EEG. These two features-diminished power spectrum in the upper alpha band at O1 and elevated approximate entropy at Cz emerged as crucial indicators that effectively differentiate between the neural signatures of healthy individuals and heroin addicts. The implications of these findings are profound, offering new avenues for the application of EEG in the diagnosis and understanding of heroin addiction. By leveraging these specific EEG features, we can enhance our ability to identify and monitor the neurological effects of heroin use, thereby contributing to more targeted and effective interventions. This study not only advances our understanding of the brain's response to heroin addiction but also underscores the potential of EEG as a powerful tool in the realm of neuropsychological assessment and addiction research.

Table 8. Comparison of accuracy and accuracy of classification.

Method	Precision	Accuracy
[51]	73.00	81.00
Time domain feature (approximate entropy in channel 11)	91.50	91.81
Frequency feature (upper alpha band in channel15)	92.95	92.40

Ethical approval

The research study was approved by the Ethics Committee of Najafabad (Approval Number: IR.IAU.NAJAFABAD.REC.1397.058).

Authors contributions

Authors have contributed equally in preparing and writing the manuscript.

Availability of data and materials

Data underlying the results presented in this paper are available from the corresponding author upon reasonable request.

Conflict of interests

The authors declare that they have no known competing financial interests or personal relationships that could have appeared to influence the work reported in this paper.

References

- [1] M. Corominas-Roso, I. Ibern, M. Capdevila, R. Ramon, C. Roncero, and J. Ramos-Quiroga. "Benefits of EEG-neurofeedback on the modulation of impulsivity in a sample of cocaine and heroin long-term abstinent inmates: a pilot study". *International Journal of Offender Therapy and Comparative Criminology*, 64(12):1275–1298, 2020.
DOI: <https://doi.org/10.1177/0306624X2090470.4>.
- [2] N. Marvi, J. Haddadnia, and M. R. F. Bordbar. "Evaluation of drug abuse on brain function using power spectrum analysis of electroencephalogram signals in methamphetamine, opioid, cannabis, and multi-drug abuser groups". *Journal of Biomedical Physics and Engineering*, 13(2):181–192, 2023.
DOI: <https://doi.org/10.31661/jbpe.v0i0.2210-1550>.
- [3] M. R. Yousefi, A. Dehghani, and H. Taghaavifar. "Enhancing the accuracy of electroencephalogram-based emotion recognition through Long Short-Term Memory recurrent deep neural networks". *Frontiers in Human Neuroscience*, 17(1174104), 2023.
- [4] M. N. Dar, M. U. Akram, R. Yuvaraj, S. G. Khawaja, and M. Murugappan. "EEG-based emotion charting for Parkinson's disease patients using Convolutional Recurrent Neural Networks and cross dataset learning". *Computers in Biology and Medicine*, 144(105327), 2022.
DOI: <https://doi.org/10.1016/j.comp-biomed.2022.105327>.
- [5] Z. M. Hira and D. F. Gillies. "A review of feature selection and feature extraction methods applied on microarray data". *Advances in Bioinformatics*, 2015(98363), 2015.
DOI: <https://doi.org/10.1155/2015/198363>.
- [6] R. V. Wankar, P. Shah, and R. Sutar. "Feature extraction and selection methods for motor imagery EEG signals: A review". *IEEE/I2C2*, pages 1–9, 2017.
DOI: <https://doi.org/10.1109/I2C2.2017.8321831>.
- [7] V. Bolón-Canedo, N. Sánchez-Marroño, A. Alonso-Betanzos, J. M. Benítez, and F. Herrera. "A review of microarray datasets and applied feature selection methods". *Information Sciences*, 282:111–135, 2014.
DOI: <https://doi.org/10.1016/j.ins.2014.05.042>.
- [8] W. Chen, Y. Cai, A. Li, Y. Su, and K. Jiang. "EEG feature selection method based on maximum information coefficient and quantum particle swarm". *Scientific Reports*, 13(14515), 2023.
DOI: <https://doi.org/https://doi.org/10.1038/s41598-023-41682-5>.
- [9] R. Sharma and H. K. Meena. "Emerging trends in EEG signal processing: A systematic review". *SN Computer Science*, 5(415), 2024.
DOI: <https://doi.org/10.1007/s42979-024-02773-w>.
- [10] A. Jain, R. Raja, S. Srivastava, P. C. Sharma, J. Gangrade, and R. Manoj. "Analysis of EEG signals and data acquisition methods: a review". *Computer Methods in Biomechanics and Biomedical Engineering: Imaging and Visualization*, 12(1), 2024.
DOI: <https://doi.org/10.1080/21681163.2024.2304574>.
- [11] M. Aziz, J. Dirkaoui, M. Ertel, M. Chakkouch, and F. Elomari. "The contribution of numerical EEG analysis for the study and understanding of addictions with substances". *International Journal of Advanced Computer Science and Applications*, 14(5), 2023.
DOI: <https://doi.org/10.14569/IJACSA.2023.0140534>.
- [12] N. Pandria, L. Kovatsi, A. B. Vivas, and P. D. Bamidis. "Resting-state abnormalities in heroin-dependent individuals". *Neuroscience*, 378:113–145, 2018.
DOI: <https://doi.org/10.1016/j.neuroscience.2016.11.018>.
- [13] M. Montazeri, M. R. Yousefi, K. Shojaei, and G. Shahgholianm. "Fast adaptive fuzzy terminal sliding mode control of synergistic movement of the hip and knee joints (air-stepping) using functional electrical stimulation: A simulation study". *Biomedical Signal Processing and Control*, 66:102445, 2021.
DOI: <https://doi.org/10.1016/j.bspc.2021.102445>.
- [14] T. Zeng, S. Li, L. Wu, Z. Feng, X. Fan, J. Yuan, X. Wang, J. Meng, H. Ma, G. Zeng, C. Kang, and J. Yang. "A Comparison study of impulsiveness, cognitive function, and P300 components between gamma-hydroxybutyrate and heroin-addicted patients: preliminary findings". *Frontiers in Human Neuroscience*, 16(16:835922), 2022.
DOI: <https://doi.org/10.3389/fnhum.2022.835922>.
- [15] H. Zeng, B. Yang, X. Gu, Y. Li, X. Xia, and S. Gao. "CNN-based EEG classification method for drug use detection". *Proceedings of the ICCPR*, pages 418–423, 2022.
DOI: <https://doi.org/10.1145/3581807.3581868>.
- [16] X. Liang, Y. Hao, Z. Xu, N. Li, and Q. Zhao. "Identifying abstinent heroin addicts on the basis of single channel's ERP and behavioral data in the gambling task". *Proceeding of the IEEE/BIBM*, pages 650–656, 2020.
DOI: <https://doi.org/10.1109/BIBM49941.2020.9313164>.
- [17] G. Y. Wang, R. Kydd, T. A. Wouldes, M. Jensen, and B. R. Russell. "Changes in resting EEG following methadone treatment in opiate addicts". *Clinical Neurophysiology*, 126(5):943–950, 2015.
DOI: <https://doi.org/10.1016/j.clinph.2014.08.021>.
- [18] N. Shourie, M. Firoozabadi, and K. Badie. "Neurofeedback training protocols based on spectral EEG feature subset and channel selection for performance enhancement of novice visual artists". *Biomedical Signal Processing and Control*, 43:117–129, 2018.
DOI: <https://doi.org/10.1016/j.bspc.2018.02.017>.
- [19] K. Jurewicz, K. Paluch, E. Kublik, J. Rogala, M. Mikicin, and A. Wróbel. "EEG-neurofeedback training of beta band (12-22 Hz) affects alpha and beta frequencies-A controlled study of a healthy population". *Neuropsychologia*, 108:13–24, 2018.
DOI: <https://doi.org/10.1016/j.neuropsychologia.2017.11.021>.
- [20] I. H. Franken, C. J. Stam, V. M. Hendriks, and W. V. D. Brink. "Neurophysiological evidence for abnormal cognitive processing of drug cues in heroin dependence". *Psychopharmacology*, 170:205–212, 2003.
DOI: <https://doi.org/https://doi.org/10.1007/s00213-003-1542-7>.
- [21] B. Hu, Q. Dong, Y. Hao, Q. Zhao, J. Shen, and F. Zheng. "Effective brain network analysis with resting-state EEG data: A comparison between heroin abstinent and non-addicted subjects". *Journal of Neural Engineering*, 14(4):046002, 2017.
DOI: <https://doi.org/10.1088/1741-2552/aa6c6f>.
- [22] Q. M. Liu, M. Lucas, F. Badami, W. Wu, A. Etkin, and T. F. Yuan. "Cortical plasticity differences in substance use disorders". *Fundamental Research*, 2023.
DOI: <https://doi.org/10.1016/j.fmre.2023.02.015>.

- [23] A. Turnip, K. D. Esti, M. F. Amri, A. I. Simbolon, M. A. Suhendra, S. Iskandar, and F. F. Wirakusumah. "Detection of drug effects on brain activity using EEG-P300 with similar stimuli". *IOP Conference Series: Materials Science and Engineering*, (012042), 2017.
DOI: <https://doi.org/10.1088/1757-899X/220/1/012042>.
- [24] F. Motlagh, F. Ibrahim, R. Rashid, T. Seghatoleslam, and H. Habil. "Investigation of brain electrophysiological properties among heroin addicts: quantitative eeg and event-related potentials.". *Journal of Neuroscience Research*, 95(8):1633–1646, 2017.
DOI: <https://doi.org/10.1002/jnr.23988>.
- [25] A. Turnip, S. M. Agung, E. K. Dwi, L. S. Faza, W. L. Simon, A. S. Siti, N. I. Arifah, and S. P. Daniel. "Methadone effects on frontal brain lobe based EEG-P300 waves in drug rehabilitation patients.". *Proceedings of the ICAE*, pages 5–11, 2020.
DOI: <https://doi.org/10.5220/0010350600050011>.
- [26] F. Motlagh, F. Ibrahim, R. Rashid, N. Shafiabady, T. Seghatoleslam, and H. Habil. "Acute effects of methadone on EEG power spectrum and event-related potentials among heroin dependents.". *Psychopharmacology*, 235:3273–3288, 2018.
DOI: <https://doi.org/10.1007/s00213-018-5035-0>.
- [27] M. Y. Badr, E. A. Gad, A. A. Mubarak, Y. A. El-Heneedy, A. M. Ibrahim, A. A. E. Belal, and F. A. E. Deep. "Impact of tramadol and heroin abuse on electroencephalography structure and cognitive functions.". *Middle East Current Psychiatry*, 30(1), 2023.
DOI: <https://doi.org/10.1186/s43045-023-00365-7>.
- [28] J. Wang, R. Peng, Q. Liu, and H. Peng. "A hybrid classification to detect abstinent heroin-addicted individuals using EEG microstates.". *IEEE Trans. on Computational Social Systems*, 9(3): 700–709, 2022.
DOI: <https://doi.org/10.1109/TCSS.2021.3135425>.
- [29] I. H. Franken, C. J. Stam, V. M. Hendriks, and W. V. D. Brink. "Electroencephalographic power and coherence analyses suggest altered brain function in abstinent male heroin-dependent patients.". *Neuropsychobiology*, 49(2):105–110, 2004.
DOI: <https://doi.org/10.1159/000076419>.
- [30] J. Luo, R. Yang, W. Yang, C. Duan, Y. Deng, J. Zhang, J. Chen, and J. Liu. "Increased amplitude of low-frequency fluctuation in right angular gyrus and left superior occipital gyrus negatively correlated with heroin use.". *Frontiers in Psychiatry*, 11:492, 2020.
DOI: <https://doi.org/10.3389/fpsy.2020.00492>.
- [31] D. M. Davydov and A. G. Polunina. "Heroin abusers' performance on the Tower of London Test relates to the baseline EEG alpha2 mean frequency shifts.". *Progress in Neuro-Psychopharmacology and Biological Psychiatry*, 28(7):1143–1152, 2004.
DOI: <https://doi.org/10.1016/j.pnpbp.2004.06.006>.
- [32] A. G. Polunina and D. M. Davydov. "EEG spectral power and mean frequencies in early heroin abstinence.". *Progress in Neuro-Psychopharmacology and Biological Psychiatry*, 28(1):73–82, 2004.
DOI: <https://doi.org/10.1016/j.pnpbp.2003.09.022>.
- [33] M. Seif, M. R. Yousefi, and N. Behzadfar. "EEG Spectral Power Analysis: A Comparison Between Heroin Dependent and Control Groups.". *Clinical EEG and Neuroscience*, 53(4):307–315, 2022.
DOI: <https://doi.org/10.1177/1550-0594221089366>.
- [34] S. N. S. Kbah, N. K. Al-Qazzaz, S. H. Jaafer, and M. K. Sabir. "Epileptic EEG activity detection for children using entropy-based biomarkers.". *Neuroscience Informatics*, 2(4), 2022.
DOI: <https://doi.org/10.1016/j.neuri.2022.100101>.
- [35] A. Cacciotti, C. Pappalettera, F. Miraglia, P. M. Rossini, and F. Vecchio. "EEG entropy insights in the context of physiological aging and Alzheimer's and Parkinson's diseases: A comprehensive review.". *GeroScience*, pages 1–21, 2021.
DOI: <https://doi.org/10.1007/s11357-024-01185-1>.
- [36] C. Bandt. "A new kind of permutation entropy used to classify sleep stages from invisible EEG microstructure.". *Entropy*, 19(5): 197, 2017.
DOI: <https://doi.org/10.3390/e19050197>.
- [37] N. S. Amer and S. B. Belhaouari. "EEG signal processing for medical diagnosis, healthcare, and monitoring: A comprehensive review.". *IEEE Access*, 11:143116–143142, 2023.
DOI: <https://doi.org/10.1109/ACCESS.2023.3341419>.
- [38] U. R. Acharya, H. Fujita, V. K. Sudarshan, S. Bhat, and J. E. Koh. "Application of entropies for automated diagnosis of epilepsy using EEG signals: A review.". *Knowledge-based systems*, 88: 85–96, 2015.
DOI: <https://doi.org/10.1016/j.knsys.2015.08.004>.
- [39] V. S. Marks, K. V. Saboo, Ç. Topçu, M. Lech, T. P. Thayib, P. Nedjedly, V. Kremen, G. A. Worrell, and M. T. Kuciewicz. "Independent dynamics of low, intermediate, and high frequency spectral intracranial EEG activities during human memory formation.". *NeuroImage*, 245(118637), 2021.
DOI: <https://doi.org/10.1016/j.neuroimage.2021.118637>.
- [40] M. R. Yousefi, A. Dehghani, S. Golnejad, and M. M. Hosseini. "Comparing EEG-based epilepsy diagnosis using neural networks and wavelet transform.". *Applied Sciences*, 13(18), 2023.
- [41] S. Moaveninejad, V. D'Onofrio, F. Tecchio, F. Ferracuti, S. Iarlori, A. Monteriù, and C. Porcaro. "Fractal Dimension as a discriminative feature for high accuracy classification in motor imagery EEG-based brain-computer interface.". *Computer Methods and Programs in Biomedicine*, 244, 2024.
DOI: <https://doi.org/10.1016/j.cmpb.2023.107944>.
- [42] D. Puri, S. Nalbalwar, A. Nandgaonkar, and A. Wagh. "EEG-based diagnosis of alzheimer's disease using kolmogorov complexity.". *Advances in Intelligent Systems and Computing*, 1354:157–165, 2021.
DOI: <https://doi.org/10.1007/978-981-16-2008-9-15>.
- [43] U. Lal, A. V. Chikkankod, and L. Longo. "Fractal dimensions and machine learning for detection of Parkinson's disease in resting-state electroencephalography.". *Neural Comput and Applic*, 36: 8257–8280, 2024.
DOI: <https://doi.org/10.1007/s00521-024-09521-4>.
- [44] S. Motamedi-Fakhr, M. Moshrefi-Torbati, M. Hill, C. M. Hill, and P. R. White. "Signal processing techniques applied to human sleep EEG signals- A review.". *Biomedical Signal Processing and Control*, 10:21–33, 2014.
DOI: <https://doi.org/10.1016/j.bspc.2013.12.003>.
- [45] Y. Liu, Y. Chen, G. Fraga-González, V. Szpak, J. Laverman, R. W. Wiers, and K. R. Ridderinkhof. "Resting-state EEG, substance use and abstinence after chronic use: A systematic review.". *Clinical EEG and Neuroscience*, 53(4):344–366, 2022.
DOI: <https://doi.org/10.1016/j.psychres.2022.111447>.
- [46] R. Alper, R. J. Chabot, A. H. Kim, L. S. Pritchep, and E. R. John. "Quantitative EEG correlates of crack cocaine dependence.". *Psychiatry Research: Neuroimaging*, 35(2):95–105, 1990.
DOI: [https://doi.org/10.1016/0925-4927\(90\)90013-V](https://doi.org/10.1016/0925-4927(90)90013-V).
- [47] M. Shen, H. Niu, Q. Xia, B. Zou, Y. Zheng, Y. Zhao, L. Li, X. Liu, and L. Zhang. "Automatic epileptic tissue localization through spatial pattern clustering of high frequency activity.". *IEEE Trans. on Neural Systems and Rehabilitation Engineering*, 31:981–990, 2023.
DOI: <https://doi.org/10.1109/TNSRE.2023.3237226>.
- [48] U. Talukdar, S. M. Hazarika, and J. Q. Gan. "Adaptation of Common Spatial Patterns based on mental fatigue for motor-imagery BCI.". *Biomedical Signal Processing and Control*, 58, 2020.
DOI: <https://doi.org/10.1016/j.bspc.2019.101829>.
- [49] A. Tobieha, N. Behzadfar, M. R. Yousefi-Najafabadi, H. Mahdavi-Nasab, and G. Shahgholian. "Choosing the distinguish- ing frequency feature of people addicted to heroin from healthy while resting.". *Signal and Data Processing*, 19(3):49–64, 2022.
DOI: <https://doi.org/10.52547/jsdp.19.3.49>.

- [50] I. H. Franken, C. J. Stam, V. M. Hendriks, and W. V. D. Brink. **“Electroencephalographic power and coherence analyses suggest altered brain function in abstinent male heroin-dependent patients.”** *Neuropsychobiology*, 49(2):105–110, 2004. DOI: <https://doi.org/10.1159/000076419>.
- [51] J. Luo, R. Yang, W. Yang, C. Duan, Y. Deng, J. Zhang, J. Chen, and J. Liu. **“Increased amplitude of low-frequency fluctuation in right angular gyrus and left superior occipital gyrus negatively correlated with heroin use.”** *Frontiers in Psychiatry*, 11, 2020. DOI: <https://doi.org/10.3389/fpsy.2020.00492>.